Activation of CD8$^+$ T Cells Contributes to Antitumor Effects of CDK4/6 Inhibitors plus MEK Inhibitors

Jessica L.F. Teh[1], Dan A. Erkes[1], Phil F. Cheng[2], Manoela Tiago[1], Nicole A. Wilski[1], Conroy O. Field[1], Inna Chervoneva[3,4], Mitch P. Levesque[2], Xiaowei Xu[5], Reinhard Dummer[2], and Andrew E. Aplin[1,4]

ABSTRACT

Concurrent MEK and CDK4/6 inhibition shows promise in clinical trials for patients with advanced-stage mutant *BRAF*/*NRAS* solid tumors. The effects of CDK4/6 inhibitor (CDK4/6i) in combination with BRAF/MEK-targeting agents on the tumor immune microenvironment are unclear, especially in melanoma, for which immune checkpoint inhibitors are effective in approximately 50% of patients. Here, we show that patients progressing on CDK4/6i/MEK pathway inhibitor combinations exhibit T-cell exclusion. We found that MEK and CDK4/6 targeting was more effective at delaying regrowth of mutant *BRAF* melanoma in immunocompetent versus immune-deficient mice. Although MEK inhibitor (MEKi) treatment increased tumor immunogenicity and intratumoral recruitment of CD8$^+$ T cells, the main effect of CDK4/6i alone and in combination with MEKi was increased expression of CD137L, a T-cell costimulatory molecule on immune cells. Depletion of CD8$^+$ T cells or blockade of the CD137 ligand–receptor interaction reduced time to regrowth of melanomas in the context of treatment with CDK4/6i plus MEKi treatment *in vivo*. Together, our data outline an antitumor immune-based mechanism and show the efficacy of targeting both the MEK pathway and CDK4/6.

Introduction

Although targeted therapies and immune checkpoint inhibitors (ICI) are FDA approved for treatment of late-stage cutaneous melanoma, challenges remain. The combination of BRAF inhibitors (BRAFi) and MEK inhibitors (MEKi) produces response in 63%–75% of patients and 14.9 months median progression-free survival (1). ICIs such as anti-CTLA4, anti–PD-1, and anti–PD-L1 elicit durable tumor regression but many patients with melanoma do not respond and/or suffer immune-related adverse effects (2, 3). Combination strategies that modulate the tumor immune microenvironment or leverage the durability of ICI could overcome the short-term efficacy of targeted therapies (4).

Aberrant G_1–S cell-cycle progression in melanoma is driven by multiple mechanisms. Highly selective CDK4/6 inhibitors (CDK4/6i) are currently FDA approved for estrogen receptor–positive (ER$^+$) breast cancer in combination with hormone signaling blockade (5). In melanoma, the combination BRAFi and/or MEKi plus CDK4/6i shows promise in preclinical mouse models (6–9). Furthermore, the addition of CDK4/6i (ribociclib) to MEKi (binimetinib) improved response rates in patients with mutant *NRAS* melanoma by more than 2-fold compared with MEKi alone (10).

Tumor-infiltrating lymphocytes (TIL) regulate tumor progression and response to therapies (11). In addition to direct effects on the tumor, CDK4/6i may also alter the tumor immune microenvironment through upregulation of coinhibitory/stimulatory molecules such as PD-L1 and MHC class I (MHC-I), release of tumor-secreted cytokines, and suppression of immune-suppressive populations such as regulatory T cells (12–15). MEKi alone promotes infiltration of CD8$^+$ T cells into the tumor but may impair T-cell priming and effector functions (16). Effects of combined MEK pathway and CDK4/6 targeting on the tumor immune microenvironment are not well understood. We therefore sought to elucidate the effects of combined treatment on different immune cell populations.

Materials and Methods

Cell lines

Mouse D4M3.A cells (donated by Dr. Constance E. Brinckerhoff, Dartmouth University, Hanover, NH, 2016) were cultured in DMEM/F12 advanced with 5% FBS, 1% penicillin/streptomycin, and 1% L-glutamine (17). Human 1205Lu cells (donated by Meenhard Herlyn, The Wistar Institute, Philadelphia, PA, 2005) were grown in WM media (MCDB153 with 2% FBS, 10% Leibowtiz L-15 medium, 5 μg/mL insulin). Human SKMEL207 cells (donated by David Solit, Memorial Sloan Kettering Cancer Center, New York, NY, 2010) were cultured in RPMI with 10% FBS. Cells were validated by short tandem repeat analysis using the Genomics Facility at The Wistar Institute. The *BRAF* mutational status of human melanoma cells lines used was confirmed by Sanger sequencing. Cell lines were tested for *Mycoplasma* contamination every 2 months using the MycoScope Kit (Genlantis).

Western blot analysis

Protein lysates were prepared in Laemmli sample buffer, separated by SDS-PAGE, and proteins were transferred to polyvinylidene difluoride membranes. Immunoreactivity was detected using horseradish peroxidase–conjugated secondary antibodies (CalBioTech) and chemiluminescence substrate (Thermo Fisher Scientific) on a Versadoc Imaging System (Bio-Rad). Primary antibodies were as follows: anti–PD-L1 (sc-19095, Santa Cruz Biotechnology) and ERK2 (sc-1647, Santa Cruz Biotechnology); anti–PD-L1 (human #13684,

[1]Department of Cancer Biology, Thomas Jefferson University, Philadelphia, Pennsylvania. [2]Department of Dermatology, University of Zurich Hospital, Zurich, Switzerland. [3]Division of Biostatistics, Department of Pharmacology and Experimental Therapeutics, Thomas Jefferson University, Philadelphia, Pennsylvania. [4]Sidney Kimmel Cancer Center, Thomas Jefferson University, Philadelphia, Pennsylvania. [5]Department of Pathology and Laboratory Medicine, Perelman School of Medicine, University of Pennsylvania, Philadelphia, Pennsylvania.

Note: Supplementary data for this article are available at Cancer Immunology Research Online (http://cancerimmunolres.aacrjournals.org/).

Corresponding Author: Andrew E. Aplin, Sidney Kimmel Cancer Center, Thomas Jefferson University, 233 South 10th Street, Philadelphia, PA 19107. Phone: 215-503-7296; Fax: 215-923-9248; E-mail: Andrew.Aplin@Jefferson.edu

Cancer Immunol Res 2020;8:1114–21

doi: 10.1158/2326-6066.CIR-19-0743

Cell Signaling Technology), anti–phospho-RB1 (S780, #9307, Cell Signaling Technology) and (S807/811, #9308, Cell Signaling Technology), anti-HSP90 (#4877, Cell Signaling Technology), phospho-ERK1/2 (T202/Y204, #9101, Cell Signaling Technology), and anti-actin (A2066, Sigma).

In vivo experiments

All studies were reviewed and approved by the Institutional Animal Care and Use Committee at Thomas Jefferson University (Philadelphia, PA). Male C57BL/6 mice (Jackson Labs) and NSG mice were used. Tumors were measured by digital caliper. Mice bearing D4M3.A tumors were fed with control chow (AIN-76A), MEKi chow (AIN-76A containing 7 ppm PD0325901), CDK4/6i chow (429 ppm palbociclib), or combination chow (AIN-76A diet with both PD0325901 and palbociclib). Combination chow was intermittently dosed for three weeks then switched to single-agent MEKi for 1 week.

Flow cytometry of tumor and spleen samples

Samples were analyzed on the BD Fortessa and data quantified with FlowJo software. Tumors were removed and dissociated into single-cell suspensions. Spleens were processed mechanically using a 70-μm nylon filter and a syringe plunger. For immunogenicity studies, cells were stained with a fixable live/dead stain (Zombie UV, BioLegend) per company instructions, fixed and permeabilized using BD Cytofix/Cytoperm Kit (BD Biosciences), followed by antibody staining. For TIL studies, cells were first stained with a fixable live/dead stain followed by surface antibody staining using the following antibodies: CD45.2 (clone 104), PD-L1 (clone 10F.9G2), IDO-1 (clone mIDO-48, eBioscience), CD137L (clone TKS-1), H-2 (MHC-I, clone M1/42), I-A/I-E (MHC-II, clone M5/114.15.1), LGalS9 (clone RG9-35), OX40L (clone RM134L), CD8α (clone 53.6.7), CD8β (clone YTS156.7.7), CD4 (clone RM4.4), NK1.1 (clone PK136), PD-1 (clone 29F.1A12), CD44 (clone IM7), CD11c (clone N418), GrzB (clone GB11, Invitrogen). For regulatory T cells (Treg) staining and Ki67 staining, cells were fixed and nuclear permeabilized using the eBioscience Foxp3/Transcription factor buffer staining set and FoxP3 antibody (clone FJK-16s) or Ki67 (clone 16A8) following manufacturer's instructions. Representative FACS plots showing gating strategy can be found in Supplementary Fig. S1.

Melanoma patient sample analysis

Patient studies were conducted according to the Declaration of Helsinki and written informed consent was obtained from all patients. Tumor samples were collected and analyzed according to University of Zurich Institutional Review Board–approved protocols (EK647 and EK800). Patient samples were collected from two clinical trials. Patients 1 and 3 were treated with LGX818 + MEK162 + LEE001, as part of the NCT01543698/CMEK162 × 2110 trial. Patient 2 was treated with LGX818 + MEK162 + LEE001 after progression on LGX818 + MEK162, as part of the NCT02159066/LOGIC2 trial. For NCT01543698, LGX818 and MEK162 were administered on a continuous schedule and LEE011 was administered in a 3-week-on, 1-week-off schedule. For NCT02159066, patients progressing on LGX818 and MEK162 were treated with LEE011. Samples were analyzed by IHC for $CD8^+$ T cells using a mouse mAb to human CD8 (clone C8/144B from Agilent). $CD8^+$ cells were counted in the entire tissue sections by imaging analysis using QuPath software (qupath.github.io). Only areas with tumor were included in the analysis. The operator was blinded to the clinical outcome.

In vivo CD8 depletion

To deplete $CD8^+$ T cells, mice were treated with 300 μg of anti-CD8α (clone 53-6.72, BioXCell) every 3 days for the duration of the experiment, starting 2 days before tumor implantation. Mouse IgG2a antibody (clone 2A3, BioXCell) was used as a control. An intermittent dosing schedule was used in which mice were fed chow dosed with a combination CDK4/6i + MEKi for 3 weeks and then switched to chow dosed with only MEKi for 1 week.

In vivo CD137L blocking

To block CD137–CD137L interactions, we utilized anti-CD137L (clone TKS-1). IgG2a isotype (clone 2A3) served as the control. Mice were treated with blocking antibody 2 days before tumor implantation and treatment was continued every 3 days. An intermittent dosing schedule was used in which mice were fed combination CDK4/6i + MEKi chow for 3 weeks and then switched to chow with only MEKi for 1 week.

In vivo OX40 agonist treatment

To stimulate the OX40 pathway, we utilized an agonistic antibody, anti-OX40/CD134 (Bio X Cell *InVivo*MAb #BE0031), or IgG1 isotype control (clone HRPN, Bio X Cell *InVivo*MAb #BE0088). Mice were treated twice a week with antibody on a 2-week on/off cycle. An intermittent dosing schedule was used for CDK4/6i + MEKi, as outlined above.

Statistical analysis of tumor growth

The statistical software used was SAS 9.4 (SAS Institute Inc.) and R 4.0.0 (R Foundation for Statistical Computing, Vienna, Austria). The log-transformed tumor volumes were analyzed using the longitudinal linear mixed effects (LME) model with quadratic time trends separate for each treatment group and random effects of an animal. Thus, the fixed effects in the LME model included the treatment group, day and day squared (day^2) as well as the interaction between the treatment group and day and day^2. All tests were two-tailed. Separate models were fitted for data from C57BL/6 and NSG experiments. The residuals were evaluated to validate the assumptions of the models. On the basis of the fitted LME models, the overall comparisons of treatment groups were performed in terms of the growth rates (testing the global null hypotheses that linear and quadratic coefficients in the quadratic function of day are equal for the compared treatment groups). Standard thresholds of $P < 0.05$ were used for significance. The P values were adjusted for multiple testing using the method of Hochberg that controls for family-wise type I error.

Results

T cells were excluded in patients who progressed on combined therapy

We have previously shown that acquired resistance to the combination of inhibitors targeting BRAF/MEK plus CDK4/6 occurred via multiple genetic alterations including *NRAS* mutation and *PIK3CA* mutation that enhance signaling through the mTOR–pS6 pathway (8, 9). However, effects on tumor-associated immune cells have not been studied in CDK4/6i-resistant melanoma. A limited number of CDK4/6i-treated mutant *BRAF* melanoma samples are available (9). Analysis of patient samples from two tumors that progressed within one year on BRAFi + MEKi + CDK4/6i therapy showed decreased $CD8^+$ T-cell infiltration compared with the pretreatment patient-matched samples (**Fig. 1A**). Both patients also demonstrated upregulation of phospho-S6 expression within their progressing tumors (9). In contrast, samples from a patient who showed a prolonged response to BRAFi + MEKi + CDK4/6i

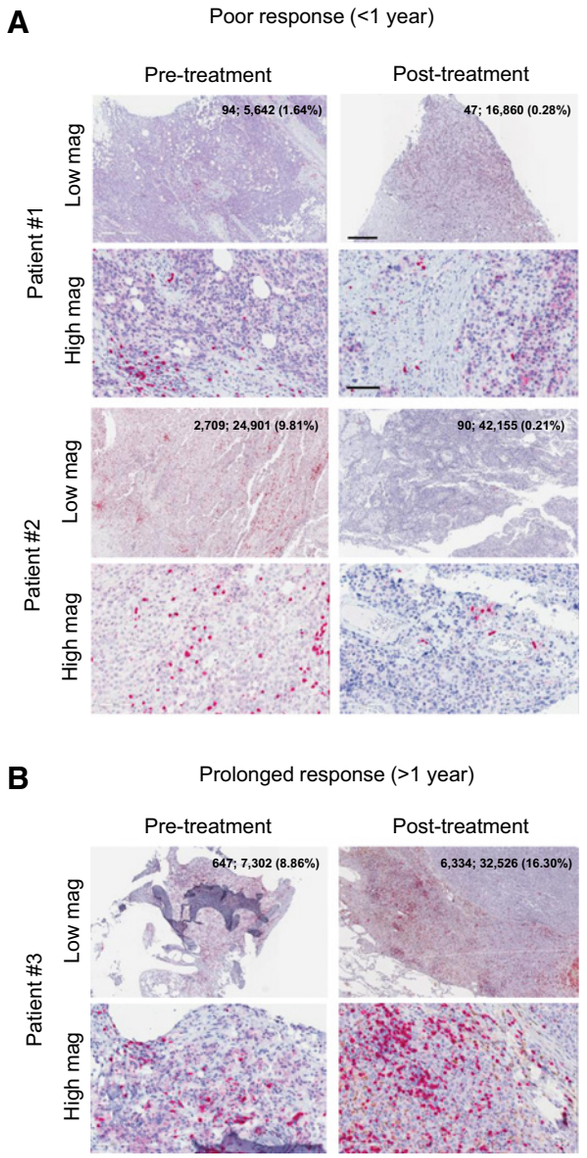

Figure 1.

T-cell exclusion in patient samples that progressed on CDK4/6i-based therapies. **A,** Immunohistochemical staining of $CD8^+$ T cells in 2 patients with ineffective responses to CDK4/6i-based treatments. Patient 1 was treated with LGX818 + MEK162 + LEE001 (CMEK162X2110 trial). Patient 2 was treated with LGX818 + MEK162 + LEE001 as part of the LOGIC2 trial. The scale bars represent 500 μM and 100 μM for low- and high-magnification images, respectively. **B,** Immunohistochemical staining of $CD8^+$ T cells in 1 patient with a prolonged response to CDK4/6i in combination with BRAF and MEK inhibitors from the CMEK162X2110 trial. Panels are similar to in **A**. The quantification of positive and negative $CD8^+$ T cells is from the low-magnification images. mag, magnification.

displayed increased $CD8^+$ T-cell staining in the posttreatment sample (**Fig. 1B**). These observations were supported by blinded quantitation of the samples (**Fig. 1A** and **B**). These data prompted us to analyze temporal alterations in the tumor immune microenvironment following treatment with inhibitors to the MAPK pathway and CDK4/6.

Combination MEKi and CDK4/6i therapy is more effective in immune-competent models

To study the role of the immune system in the response and resistance to targeted therapies combination, we utilized the *Braf* ^{V600E}/*Pten* loss D4M3.A mouse melanoma model (17). We focused on CDK4/6i combined with MEKi because this pairing is broadly applicable across many melanoma subtypes with encouraging early clinical data (18, 19) and our previous work has shown the on-target effects of this combination (7, 9). Treatment of D4M3.A cells with MEKi and CDK4/6i *in vitro* decreased phospho-ERK1/2 and phospho-RB1 amounts, respectively (**Fig. 2A**).

We have previously shown MEKi plus CDK4/6i reduced E2F-driven transcription using *in vivo* reporter models in immune-compromised mice (7). Next, we tested effects in mouse melanoma models. D4M3.A cells were injected into either immune-compromised NOD-*scid* γ (NSG) mice or immunocompetent syngeneic C57BL/6 mice. Once tumors were formed, mice were treated with chow laced with either vehicle, MEKi alone, CDK4/6i alone, or the combination of MEKi plus CDK4/6i. An intermittent, 3 weeks on/1 week off schedule was used for CDK4/6i, consistent with clinical use. In immune-compromised NSG mice, MEKi alone, and combination treatment led to tumor regressions, whereas CDK4/6i alone elicited little effect (**Fig. 2B**). However, tumors in both MEKi alone and MEKi plus CDK4/6i combination arms rapidly acquired resistance after 17 days of treatment and the mice had to be sacrificed within 24 and 28 days, respectively. Tumor regressions following MEKi alone and MEKi plus CDK4/6i treatment also occurred in C57BL/6 mice but, in contrast to tumors in NSG mice, there was a more durable inhibition of tumor growth (**Fig. 2C**). MEKi-treated mice survived up to 38–43 days, whereas MEKi plus CDK4/6i-treated mice survived up to 43–52 days (**Fig. 2C**). CDK4/6i alone had little to no effect on tumor growth inhibition in either NSG or C57BL/6 mice. Control tumors grew with an average growth rate of 8.6% per day (95% CI: 7.6%–9.7%) in C57BL/6 mice compared with an average of 10.0% per day (95% CI: 8.4%–11.7%) in NSG mice (**Fig. 2B** and **C**). The overlap between these two 95% confidence intervals (8.4%–9.7%) provides evidence that the growth rates of untreated tumors are similar in C57BL/6 and NSG mice. Together, these data suggest that the immune system plays a role in the efficacy of MEKi and CDK4/6i with MEKi being the main mediator of response in this model.

$CD8^+$ T cells are required for the efficacy of MEKi and CDK4/6i combination therapy

To determine the mechanism by which the immune system contributes to the antitumor effects of MEKi and CDK4/6i, we treated D4M3.A allografts for four days and profiled changes in immune cell populations. We detected significant upregulation of both MHC-I and MHC-II expression with MEKi plus CDK4/6i treatment, suggesting increased antigen presentation (**Fig. 3A**; Supplementary Fig. S1). $CD8^+$ T cells were associated with MHC-I expression and were significantly increased within the tumor with both MEKi treatment alone and combination MEKi plus CDK4/6i treatment (**Fig. 3B**). No significant changes were detected in $CD4^+$ T cells, $FOXP3^+$ regulatory T cells (Tregs), or natural killer (NK) cells within the tumor (**Fig. 3B**; Supplementary Figs. S1, S2A, and S2B). *In vitro*, we observed a more pronounced modulation of HLA-ABC expression in mutant *BRAF* and mutant *NRAS* human melanoma cell lines treated with MEKi plus CDK4/6i compared with single-agent treatments (**Fig. 3C**; Supplementary Fig. S1).

Because $CD8^+$ T cells infiltrated into the tumor, we performed phenotypic analysis of this population. There were moderate but

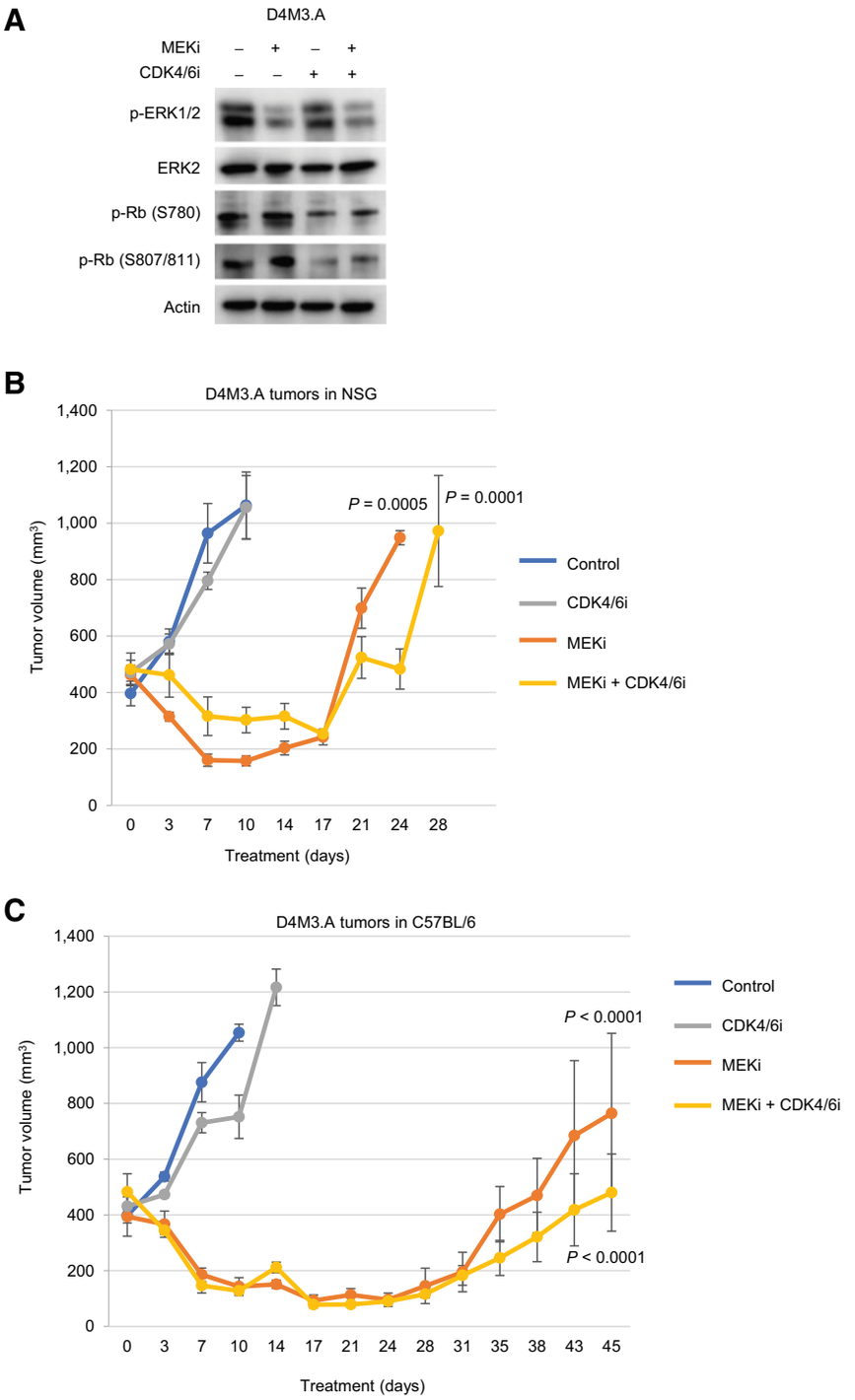

Figure 2.

Combined MEKi and CDK4/6i therapy is more effective than either alone in immunocompetent mouse models. **A,** Braf^{V600E}-mutant D4M3.4 cells were treated with DMSO (vehicle control), MEKi (PD0325901, 10 nmol/L) alone, CDK4/6i (palbociclib, 1 μmol/L) alone, and combination treatment *in vitro* for 72 hours. Analysis of downstream targets was performed by Western blot analysis. Representative blots from three independent experiments are shown. **B,** NSG mice were intradermally implanted with the mouse *Braf* ^{V600E} melanoma cell line D4M3.A (3×10^5 cells). Tumors were grown to approximately 400 mm^3, after which animals were given control (AIN-76A)-, MEKi (PD0325901)-, CDK4/6i (palbociclib)-, and combination-laced chow. Palbociclib was dosed intermittently, 3 weeks on, 1 week off. Number of samples: control, $n = 5$; MEKi, $n = 5$; CDK4/6i, $n = 5$; and MEKi + CDK4/6i, $n = 5$. Bars, SEM. **C,** As in **B** except that C57BL/6 mice were used. Number of samples: control, $n = 4$; MEKi, $n = 4$; CDK4/6i, $n = 5$; and MEKi plus CDK4/6i, $n = 5$. *P* values are given for the MEKi and MEKi plus CDK4/6i arms compared with control arm.

nonsignificant increases in markers for proliferation (Ki67), effector/memory T-cell phenotype (CD44), and cytotoxicity (granzyme B) following MEKi treatment alone and combination MEKi plus CDK4/6i treatment (**Fig. 3D**; Supplementary Fig. S1). CDK4/6 inhibition alone did not repress proliferation of CD8$^+$ T cells (**Fig. 3D**). To determine whether CD8$^+$ T cells play a functional role in MEK and CDK4/6 targeting, we used antibody to deplete CD8$^+$ T cells in mice prior to implantation of D4M3.A melanoma tumors. We then treated the mice with MEKi plus CDK4/6i (**Fig. 3E** and **F**). Although we observed initial regression of the tumors in both IgG and CD8 depletion arms, tumors within the CD8-depleted arm progressed more rapidly and mice had to be sacrificed by day 44 (**Fig. 3E** and **F**). Although it is possible that depleting CD8$^+$ cells prior to tumor implantation alters tumor progression when compared with tumor growth in fully immunocompetent animals, the impact should be minimal as there is very little immune infiltration into the lesions without intervention. Taken

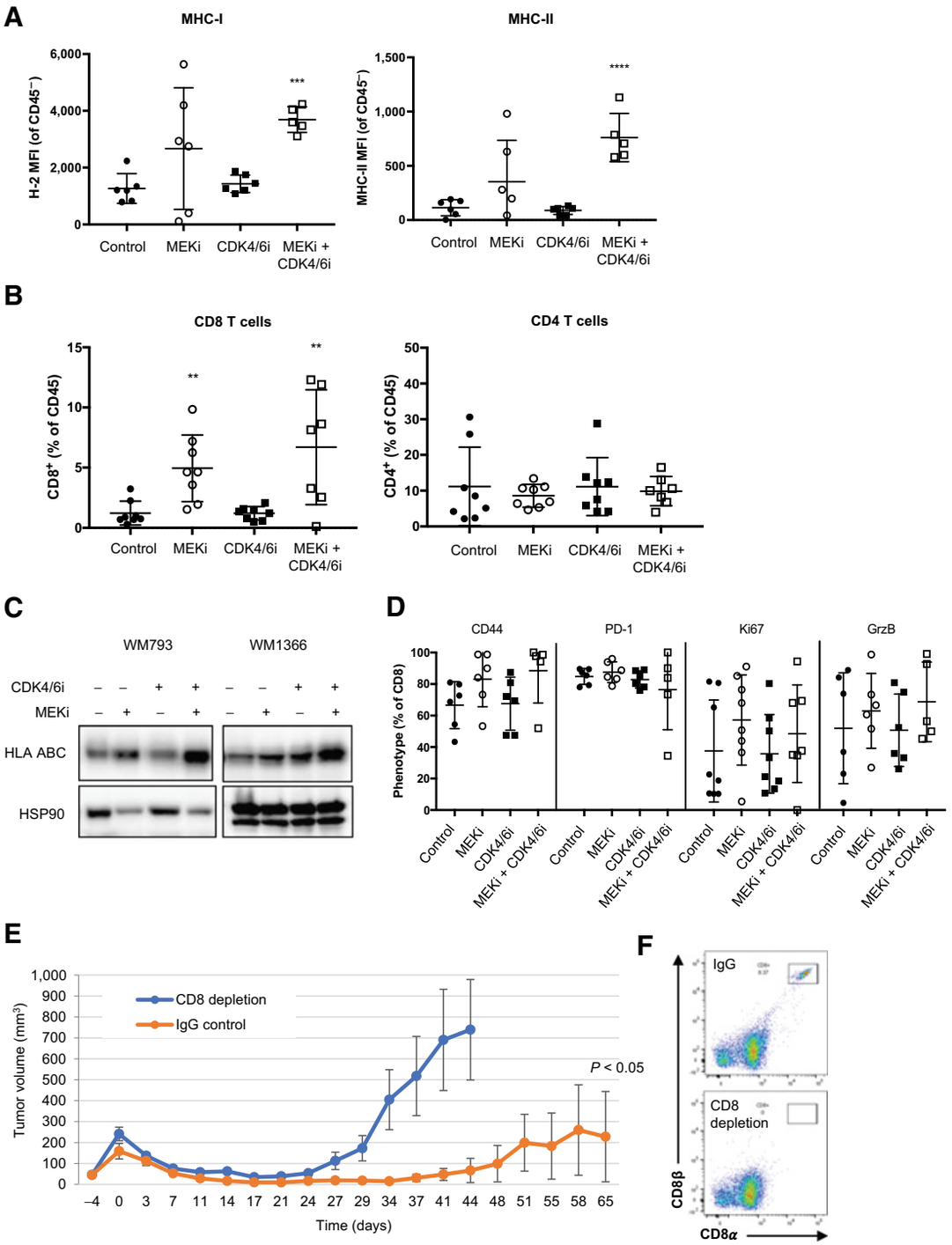

Figure 3.

MEK plus CDK4/6 inhibition leads to increased antigen presentation and recruits functional CD8$^+$ T cells to the tumor. **A,** D4M3.A mouse melanoma tumors were treated for 4 days, and cells from tumors were analyzed by flow cytometry for MHC-I levels. Graphed are mean and SD. *, $P < 0.05$; **, $P < 0.01$; ***, $P < 0.001$; ****, $P < 0.0001$. MFI, mean fluorescence intensity. **B,** CD8$^+$ expressing CD45$^+$ immune cells. *, $P < 0.05$; **, $P < 0.01$; ***, $P < 0.001$; ****, $P < 0.0001$. **C,** Human melanoma cell lines were treated with DMSO, MEKi (PD0325901, 5 nmol/L), CDK4/6i (palbociclib, 0.5 μmol/L), or MEKi plus CDK4/6i for 48 hours. Lysates were analyzed by Western blotting for MHC-I expression. **D,** CD8$^+$ T cells in **B** were phenotyped by expression of CD44$^+$, PD-1, Ki67, and granzyme B (GrzB). **E,** C57BL/6 mice were depleted of CD8 cells by intraperitoneal injection of CD8α (clone 53-6.72) antibody 3 days prior to intradermal implantation of D4M3.A cells. Tumors were grown to approximately 300 mm^3, and then mice were treated with MEKi plus CDK4/6i. Isotype rat IgG2a (clone 2A3) and CD8α antibodies were intraperitoneally injected into mice twice a week. Number of samples: IgG, $n = 4$; CD8α, $n = 6$. $P < 0.05$. Error bars, SEM. **F,** Depletions were confirmed on day 17 after MEKi plus CDK4/6i treatment by flow cytometry. Whole blood was collected and stained with a cocktail of anti-CD45.2, anti-CD8α, and CD8β for 30 minutes.

together, our data suggest a role for $CD8^+$ T cells in the antitumor immunity driven by MEKi plus CDK4/6i treatment.

CDK4/6 inhibition does not affect PD-L1 expression on melanoma or immune cells

Next, we explored whether CDK4/6i-based combinations could modulate T-cell coinhibitory molecules. PD-L1 expression is cell-cycle regulated through the RB1–NF-κB axis and ubiquitination/proteasome pathway proteins (13, 20). When analyzing D4M3.A tumors that were treated for 4 days, we did not observe modulation of PD-L1, IDO1, or LGasS9 expression in any of the treatment groups in either $CD45^-$ tumor cells or $CD45^+$ immune cells (Supplementary Figs. S1 and S3A–S3C). However, the average number of PD-L1 molecules per $CD45^+$ immune cell was decreased after MEKi alone and MEKi plus CDK4/6i combination treatment (Supplementary Figs. S1 and S3D). In human melanoma cell lines, targeting CDK4/6 did not lead to modulation of IFNγ-induced PD-L1 amounts (Supplementary Fig. S3E). Overall, these data indicate that CDK4/6 inhibition does not uniformly regulate PD-L1 expression across melanoma models.

T-cell activation markers are altered by MEK and CDK4/6 cotargeting

To further characterize the mechanisms underlying immune cell–based effects of combined MEK plus CDK4/6 targeting, we analyzed modulation of costimulatory T-cell molecules that may potentially enhance $CD8^+$ T-cell function. First, we detected downregulation of OX40 ligand (OX40L) on $CD45^+$ immune cells and $CD11c^+$ antigen-presenting cells (APC) in both the MEKi alone and in combination with CDK4/6i treatment arms (**Fig. 4A**; Supplementary Fig. S1). Effects were more marked with MEKi alone and were consistent with other reports that suggest that MEK inhibition may adversely affect long-term T-cell effector function (16, 21). On the basis of OX40L downregulation, we tested the effect of OX40 agonists on the efficacy of the MEKi plus CDK4/6i combination. D4M3.A allografts were treated with OX40 agonist or control antibody before and during MEKi plus CDK4/6i treatment. We compared tumor response, time until tumors regrew to the original size, and animal survival following initiation of treatment. Although tumors regressed in the OX40 agonist and MEKi plus CDK4/6i treatment arm and some of the regressions were durable, the time to regrowth and survival data were not significantly different between the OX40 agonist and control arms (**Fig. 4B**; Supplementary Fig S4). These data suggest that agonistic anti-OX40 did not improve MEKi and CDK4/6i therapy in the D4M3.A melanoma model. We do not rule out the possibility that OX40L agonists may elicit effects with MEKi alone.

In addition to effects on OX40L expression, we also detected a significant induction of CD137L expression on $CD11c^+$ APCs in D4M3.A allografts following CDK4/6i treatment alone and in combination with MEKi (**Fig. 4C**; Supplementary Fig. S1). CDK4/6i upregulated CD137L expression on the $CD45^+$ cell population, but this was partially antagonized by the addition of MEKi (**Fig. 4C**, middle). Nonetheless, these data suggest that CDK4/6 inhibition may enhance activation signals to $CD8^+$ T cells. To determine whether upregulation of CD137L was functionally important, we utilized a blocking antibody to CD137L in mice bearing D4M3.A melanomas and also treated mice with MEKi plus CDK4/6i. Similar to CD8 antibody–mediated depletion, D4M3.A tumor–bearing mice initially regressed in response to MEKi plus CDK4/6i treatment in both IgG control and CD137L blocking antibody arms. However, the majority of tumors in the CD137L blocking arm reached approximately 1,000 mm^3 between 34 and 45 days, and all mice had to be sacrificed by day 45 (Supplementary Fig. S4). In contrast, the IgG control group had overall smaller tumors, improved survival, and significantly delayed regrowth of residual tumors to their original size after treatment (**Fig. 4D**). Together, our data suggest that upregulation of CD137L on $CD11c^+$ APCs by CDK4/6i may contribute to the improved therapeutic outcomes of MEKi plus CDK4/6i combination.

Discussion

Our studies in a $Braf^{V600E}$/*Pten* loss syngeneic mouse model highlight two mechanisms by which MEKi plus CDK4/6i effects associate with antitumor immunity. First, MEKi plus CDK4/6i increased capacity of melanoma cells to present antigen and recruitment of cytotoxic $CD8^+$ T cells to the tumor. Second, CDK4/6 inhibition may enhance MEKi effects by sustaining the activation of infiltrating $CD8^+$ T cells, at least in part, via induction of CD137L (4-1BBL) on APCs. Although increased MHC-I and infiltration of $CD8^+$ T cells (14, 21) have previously been associated with CDK4/6 inhibition alone, a report on a KRAS-mutant lung cancer mouse model treated with combination MEKi, trametinib plus palbociclib, demonstrated that these infiltrating $CD8^+$ T cells did not bear activation markers and did not play a functional role in antitumor immunity (22). Together, our and others' findings suggest that targeted therapies have multiple effects on different cell types within the tumor microenvironment that ultimately enhance the effects of immunotherapy.

Our study shows that CDK4/6i led to increased expression of CD137L on $CD11c^+$ antigen-presenting cells. CD137L is the ligand for CD137 (4-1BB), which belongs to the TNF receptor family (TNFR9) and serves as a bona fide costimulatory molecule for T cells (23). CD137 is typically expressed after T-cell activation and ligation of CD137 leads to enhanced T-cell survival and proliferation. These functional properties of CD137 signaling are being exploited in the clinic with the use of agonistic antibodies, although their activity has been hampered by liver toxicities and potency issues (24). CD137 receptor expression is upregulated on both primary $CD4^+$ and $CD8^+$ T cells after exposure to CDK4/6i, abemaciclib (14). Our studies highlight an alternative way for providing CD137 ligation to overcome dysfunction or exhaustion of T cells. The adverse downregulation of another costimulatory molecule, OX40L (CD134/TNFRSF4), by MEKi may be compensated for by induction of CD137L from CDK4/6 inhibition (**Fig. 4E**). Together, this might lead to improved outcomes in the combination arm although more studies are required.

Loss of T-cell infiltration and dysfunction of T cells have been linked to acquired resistance to both MAPK-targeted therapies and immunotherapies (25). Our patient-based studies are complementary to such findings; however, these analyses are limited by the small number of patient-matched samples available to us and by the realization that these biopsies could have been taken from different lesions. Our results indicate that salvage therapies should be carefully selected for use in conjunction with anti–PD-1. Future studies might identify optimal sequencing of CDK4/6i-based combinations and ICI. Studies in melanoma and colorectal cancer models have suggested that phased combinations of CDK4/6i and ICI may be most effective to obtain synergism (14, 26). Overall, our data show that MEKi plus CDK4/6i combinations improve $CD8^+$ T-cell recruitment and function, and they support clinical testing in combination with immunotherapy in melanoma.

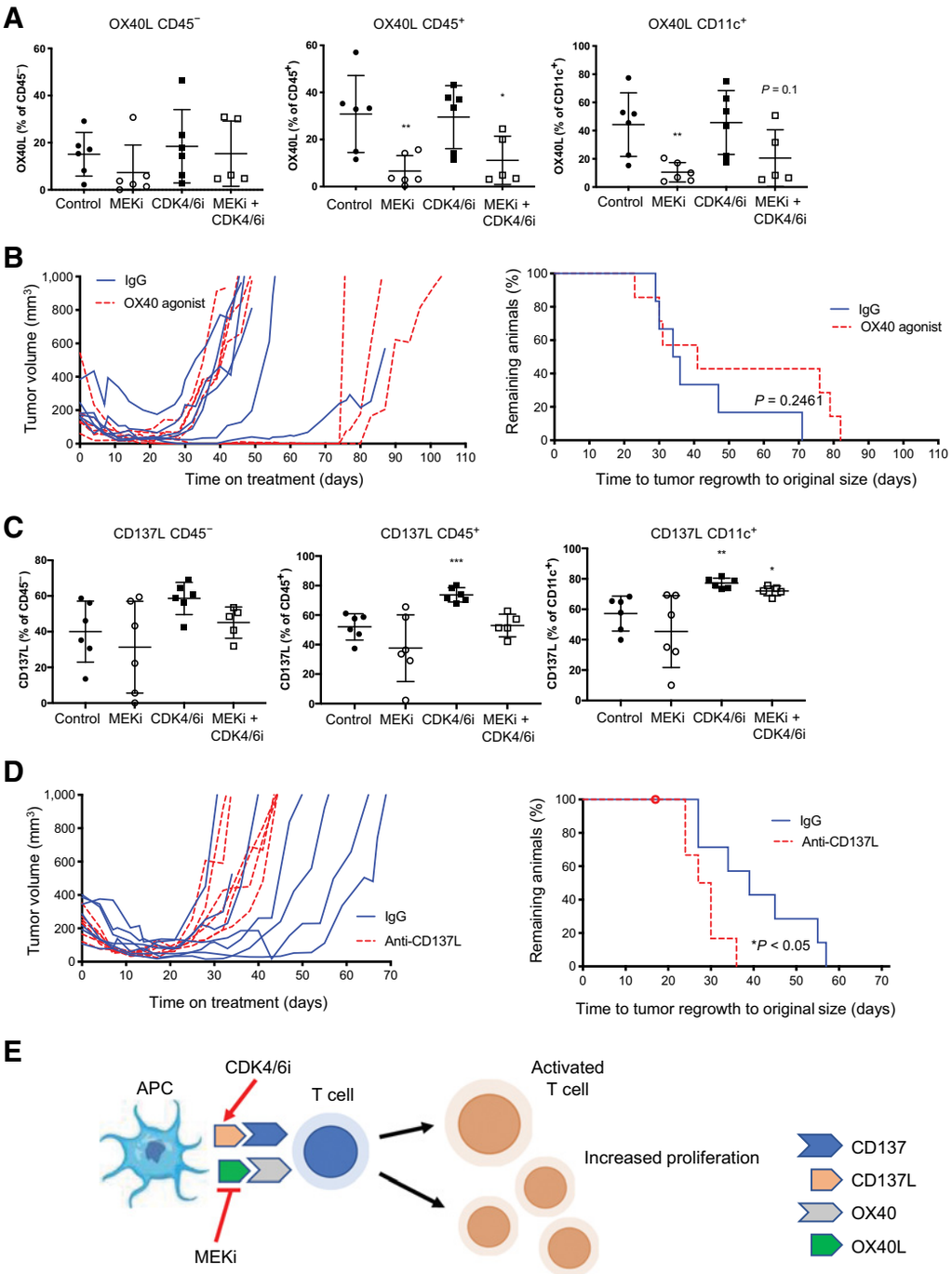

Figure 4.

T-cell costimulatory molecules are altered with MEK and CDK4/6 targeting. **A,** D4M3.A mouse melanoma tumors were treated for 4 days, and tumors were analyzed for expression of the T-cell costimulatory molecule OX40L on $CD45^-$ tumor cells, $CD45^+$ immune cells, and $CD11c^+$ APCs. Graphed are mean and SD. *, $P < 0.05$; **, $P < 0.01$; ***, $P < 0.001$; ****, $P < 0.0001$. **B,** Tumor regression following MEKi plus CDK4/6i treatment and delay of regrowth to starting size. Mice bearing tumors approximately 300 mm^3 in size were intraperitoneally injected with either OX40 agonist ($n = 7$) or the corresponding isotype control (IgG1, $n = 6$) twice a week before and during treatment with MEKi plus intermittent CDK4/6i treatment or control chow treatment. The experiment was ended when tumors were 1,000 mm^3. **C,** As for **A** except that cells were stained for CD137L. *, $P < 0.05$; **, $P < 0.01$; ***, $P < 0.001$; ****, $P < 0.0001$. **D,** As for **B** except that mice were intraperitoneally injected with CD137L blocking antibody (clone TKS-1) or the corresponding isotype control (IgG2a) 2 days prior to intradermal implantation with D4M3.A cells. Dot indicates when animals were censored due to euthanizing before tumor regrew to the original size when MEKi plus CDK4/6i treatment was started. Significance was assessed, as described in Materials and Methods, by a log-rank test, *, $P < 0.05$. **E,** Model describing actions of CDK4/6i and MEKi in melanoma tumors. The downregulation of the costimulatory molecule OX40L by MEKi may be compensated for by the CDK4/6i-mediated induction of CD137L on $CD11c^+$ APCs.

Disclosure of Potential Conflicts of Interest

J.L.F. Teh reports a patent for US 9880150B2 issued. D.A. Erkes reports that he is now an employee of the journal publisher, the American Association for Cancer Research, and had no influence over any editorial decisions related to this article. I. Chervoneva reports grants from NIH/NCI R01 CA196278 during the conduct of the study. X. Xu reports personal fees and other from CureBiotech Inc. (cofounder) and other from Exio Bioscience (cofounder) outside the submitted work. R. Dummer has intermittent, project-focused consulting and/or advisory relationships with Novartis, Merck Sharp & Dohme, Bristol-Myers Squibb, Roche, Amgen, Takeda, Pierre Fabre, Sun Pharma, Sanofi, Catalym, Second Genome, Regeneron, and Alligator outside the submitted work. A.E. Aplin reports grants from the NIH (CA196278, CA182635, CA114046, and CA236736), Dr. Miriam and Sheldon G. Adelson Medical Research Foundation, U.S. Department of Defense, Outrun the Sun, and Pfizer during the conduct of the study, as well as a patent for US 9880150 issued. No potential conflicts of interest were disclosed by the other authors.

Authors' Contributions

J.L.F. Teh: Conceptualization, data curation, funding acquisition, validation, investigation, methodology, writing–original draft, writing–review and editing. **D.A. Erkes:** Investigation, methodology, writing–original draft. **P.F. Cheng:** Resources, investigation, visualization. **M. Tiago:** Investigation. **N.A. Wilski:** Data curation, investigation, writing–review and editing. **C.O. Field:** Investigation. **I. Chervoneva:** Data curation. **M.P. Levesque:** Resources, funding acquisition, project administration. **X. Xu:** Formal analysis, investigation. **R. Dummer:** Funding acquisition, project administration. **A.E. Aplin:** Conceptualization, resources, funding acquisition, writing–original draft, project administration, writing–review and editing.

Acknowledgments

This work is supported by grants from the NIH (R01 CA196278 and R01 CA182635), and the Dr. Miriam and Sheldon G. Adelson Medical Research Foundation (to A.E. Aplin). A.E. Aplin and X. Xu are supported by an NCI P01 in Targeted Therapies in Melanoma (CA114046). X. Xu was supported by grants from the U.S. Department of Defense (CA170340) and NIH (CA210944 and CA224070). J.L.F. Teh was supported by Outrun the Sun Research Scholar Award. N.A. Wilski is supported by the T32 Training Program in Cancer Biology (CA236736). The Sidney Kimmel Cancer Center Flow Cytometry, Translational Pathology, and Meta-Omics core facilities are supported by an NCI Support Grant (P30 CA056036).

Received October 2, 2019; revised March 19, 2020; accepted June 26, 2020; published first July 13, 2020.

References

1. Dummer R, Ascierto PA, Gogas HJ, Arance A, Mandala M, Liszkay G, et al. Overall survival in patients with BRAF-mutant melanoma receiving encorafenib plus binimetinib versus vemurafenib or encorafenib (COLUMBUS): a multicentre, open-label, randomised, phase 3 trial. Lancet Oncol 2018;19:1315–27.
2. Larkin J, Chiarion-Sileni V, Gonzalez R, Grob JJ, Cowey CL, Lao CD, et al. Combined nivolumab and ipilimumab or monotherapy in untreated melanoma. N Engl J Med 2015;373:23–34.
3. Robert C, Schachter J, Long GV, Arance A, Grob JJ, Mortier L, et al. Pembrolizumab versus ipilimumab in advanced melanoma. N Engl J Med 2015;372:2521–32.
4. Sullivan RJ, Hamid O, Gonzalez R, Infante JR, Patel MR, Hodi FS, et al. Atezolizumab plus cobimetinib and vemurafenib in BRAF-mutated melanoma patients. Nat Med 2019;25:929–35.
5. Finn RS, Martin M, Rugo HS, Jones S, Im SA, Gelmon K, et al. Palbociclib and letrozole in advanced breast cancer. N Engl J Med 2016;375:1925–36.
6. Kwong LN, Costello JC, Liu H, Jiang S, Helms TL, Langsdorf AE, et al. Oncogenic NRAS signaling differentially regulates survival and proliferation in melanoma. Nat Med 2012;18:1503–10.
7. Teh JL, Purwin TJ, Greenawalt EJ, Chervoneva I, Goldberg A, Davies MA, et al. An in vivo reporter to quantitatively and temporally analyze the effects of CDK4/6 inhibitor-based therapies in melanoma. Cancer Res 2016;76:5455–66.
8. Romano G, Chen PL, Song P, McQuade JL, Liang RJ, Liu M, et al. A preexisting rare PIK3CA(E545K) subpopulation confers clinical resistance to MEK plus CDK4/6 inhibition in NRAS melanoma and is dependent on S6K1 signaling. Cancer Discov 2018;8:556–67.
9. Teh JLF, Cheng PF, Purwin TJ, Nikbakht N, Patel P, Chervoneva I, et al. In vivo E2F reporting reveals efficacious schedules of MEK1/2-CDK4/6 targeting and mTOR-S6 resistance mechanisms. Cancer Discov 2018;8:568–81.
10. Schuler MH, Ascierto PA, De Vos FYFL, Postow MA, Van Herpen CML, Carlino MS. Phase 1b/2 trial of ribociclib+binimetinib in metastatic NRAS-mutant melanoma: safety, efficacy, and recommended phase 2 dose (RP2D). J Clin Oncol 35, 2017 (suppl; abstr 9519).
11. Spranger S, Gajewski TF. Impact of oncogenic pathways on evasion of anti-tumour immune responses. Nat Rev Cancer 2018;18:139–47.
12. Goel S, DeCristo MJ, Watt AC, BrinJones H, Sceneay J, Li BB, et al. CDK4/6 inhibition triggers anti-tumour immunity. Nature 2017;548:471–5.
13. Zhang J, Bu X, Wang H, Zhu Y, Geng Y, Nihira NT, et al. Cyclin D-CDK4 kinase destabilizes PD-L1 via cullin 3-SPOP to control cancer immune surveillance. Nature 2018;553:91–5.
14. Schaer DA, Beckmann RP, Dempsey JA, Huber L, Forest A, Amaladas N, et al. The CDK4/6 inhibitor abemaciclib induces a T cell inflamed tumor microenvironment and enhances the efficacy of PD-L1 checkpoint blockade. Cell Rep 2018;22:2978–94.
15. Teh JLF, Aplin AE. Arrested developments: CDK4/6 inhibitor resistance and alterations in the tumor immune microenvironment. Clin Cancer Res 2019;25:921–7.
16. Dushyanthen S, Teo ZL, Caramia F, Savas P, Mintoff CP, Virassamy B, et al. Agonist immunotherapy restores T cell function following MEK inhibition improving efficacy in breast cancer. Nat Commun 2017;8:606.
17. Jenkins MH, Steinberg SM, Alexander MP, Fisher JL, Ernstoff MS, Turk MJ, et al. Multiple murine BRaf(V600E) melanoma cell lines with sensitivity to PLX4032. Pigment Cell Melanoma Res 2014;27:495–501.
18. Sosman J, Kittaneh M, Lolkema M, Postow M, Schwartz G, Franklin C, et al. A phase 1b/2 study of LEE011 in combination with binimetinib (MEK162) in patients with NRAS-mutant melanoma: early encouraging clinical activity. J Clin Oncol 32:5s, 2014 (suppl; abstr 9009).
19. Van Herpen C, Postow MA, Carlino MS, Kalkavan H, Weise A, Amaria RN, et al. A phase 1b/2 study of ribociclib (LEE011; CDK4/6 inhibitor) in combination with binimetinib (MEK162; MEK inhibitor) in patients with NRAS-mutant melanoma. Euro J Cancer 2015;2015:S663.
20. Jin X, Ding D, Yan Y, Li H, Wang B, Ma L, et al. Phosphorylated RB promotes cancer immunity by inhibiting NF-kappaB activation and PD-L1 expression. Mol Cell 2019;73:22–35.
21. Ebert PJR, Cheung J, Yang Y, McNamara E, Hong R, Moskalenko M, et al. MAP kinase inhibition promotes T cell and anti-tumor activity in combination with PD-L1 checkpoint blockade. Immunity 2016;44:609–21.
22. Ruscetti M, Leibold J, Bott MJ, Fennell M, Kulick A, Salgado NR, et al. NK cell-mediated cytotoxicity contributes to tumor control by a cytostatic drug combination. Science 2018;362:1416–22.
23. Chester C, Sanmamed MF, Wang J, Melero I. Immunotherapy targeting 4–1BB: mechanistic rationale, clinical results, and future strategies. Blood 2018;131:49–57.
24. Segal NH, He AR, Doi T, Levy R, Bhatia S, Pishvaian MJ, et al. Phase I study of single-agent utomilumab (PF-05082566), a 4–1BB/CD137 agonist, in patients with advanced cancer. Clin Cancer Res 2018;24:1816–23.
25. Hugo W, Shi H, Sun L, Piva M, Song C, Kong X, et al. Non-genomic and immune evolution of melanoma acquiring MAPKi resistance. Cell 2015;162:1271–85.
26. Jerby-Arnon L, Shah P, Cuoco MS, Rodman C, Su MJ, Melms JC, et al. A cancer cell program promotes t cell exclusion and resistance to checkpoint blockade. Cell 2018;175:984–97.